A 6-Port Two-Dimensional 3 × 3 Series-Fed Planar Array Antenna for Dual-Polarized X-Band Airborne Synthetic Aperture Radar Applications

VENKATA KISHORE KOTHAPUDI[ID], **(Member, IEEE), AND VIJAY KUMAR, (Member, IEEE)**
Department of Communication Engineering, School of Electronics Engineering, VIT University, Vellore 632014, India
Corresponding author: Venkata Kishore Kothapudi (v.k.kothapudi@ieee.org)

ABSTRACT A six-port 3 × 3 series-fed planar antenna array design for dual polarized X-band airborne synthetic aperture radar (SAR) applications is presented in this paper. The antenna array patches interconnected with series feeding one to another as the structure to realize directional radiation and vertical/horizontal polarization. The patch elements are excited through 50 Ω microstrip line feeding in series with quarter wave transformer for good impedance characteristics. A six-port feeding allows selecting the direction of the traveling waves, and consequently the sense of linear (vertical and horizontal) polarization. A prototype of the antenna is fabricated and validated the proposed method. The dimensions of the fabricated prototype 3 × 3 array antenna are $3.256\lambda_g \times 3.256\lambda_g \times 0.0645\lambda_g$ (λ_g is guided wavelength at center frequency 9.65 GHz). The measured $S_{11} < -10$ dB reflection bandwidths are 1.4% at each port. Furthermore, an interport and intraport isolation S21<-25 dB was also achieved across the operation band. The measured peak gains are higher than 11.5 dBi with 90% efficiency for all individual ports/polarizations V1, V2, V3 H1, H2, and H3). In order to satisfy the different performance requirement of series-fed array antenna, such as realized gain, radiation efficiency, side lobe level, half power beam width and front to back ratio are also examined. Measured results of an antenna prototype successfully validate the concept. The proposed antenna is found suitable for dual polarized airborne SAR applications.

INDEX TERMS Series-fed, antenna arrays, linear polarization, side lobe level (SLL), front to back ratio (FTBR), airborne synthetic aperture radar (ASAR).

I. INTRODUCTION

Airborne SAR (Synthetic Aperture Radar) systems is an end-to-end multimode X-band SAR systems with real-time capabilities are designed for military applications like tactical surveillance and target reconnaissance. Compact and lightweight radar system designs are perfectly suited for installation on UAVs, small aircraft, helicopters and lighter-than-air vehicles. [1]. The Dual polarized antenna is suitable for polarization diversity applications and to increase communication capacity. Proposed structure can enhance the information content by providing two co-polarized and two cross-polarized back scattered data. The SIR-C shuttle imaging radar operated at L and C-bands with dual polarization at each frequency. Antennas with diverse characteristics can be used in new generation radar systems to meet a compact design for airborne or spaceborne SAR systems. Antenna technology using dual polarization is of massive use in communication, especially in the view of the gradual increase in

demand for communication channels. Such a technology also should help in reducing a cost of antenna, weight, as well as improving radar cross section (RCS).

Efficiency of phased array system depends on the performance of low noise amplifier (LNA) and phase shifters which can be achieved with the designs of a high-performance phase shifter and LNA in CMOS technology [2]. Different antenna array schemes along with the hand effect on the antenna array at 15 GHz presented in [3]. The extended-resonance technique along with the heterodyne-mixing concept proposed in [4]. This is capable of reducing the complexity of phased arrays by eliminating separate power dividers and phase shifters. A single phase shifter and a separate gain controller for each antenna in [5] were presented to enable a low-cost and less complex phased-array system. A new electronic beam forming in a limited scan range approach that requires only a single phase shifter and a single gain controller, independent of the number of antenna elements

has been introduced [6]. Corporate feed and Series-feed networks are two possible arrangements for feeding these types of arrays presented by James *et.al* [7]. Compared with corporate arrangements, series-feed networks have the benefits of simplicity and compactness, which can translate into low-loss feeding structures proposed by Pozar *et.al* [8]. In the case of corporate feeding network, numerous power dividers containing many discontinuities and long transmission lines causes spurious radiation and significant dielectric loss. Conversely, the series-fed structure uses short transmission lines and enhances antenna efficiency presented in [9]. Improved impedance matching and radiation pattern characteristics of the series-fed arrays were presented in [10] and [11] by using a matching-in-step taper or stepped impedance linear configuration and adopting the method of the modified transmission line model in a 2-D array respectively. James *et.al* [7], demonstrated coupling mechanisms for series-fed arrays include direct (microstrip line and co-axial probe feed), proximity coupled and aperture couplings. Arrays based on direct coupling include cascaded patch arrays provided in [12] and combline antennas provided in [13]. In contrast to aperture coupling [14], direct coupling microstrip line) usually requires a simpler coplanar structure rather than a multi-layer design. Carter *et.al* [15] and Owens *et.al* [16] proposed series-fed arrays based on a coplanar proximity coupling mechanism. Recently authors reported X-band 1 × 2 linear array design with direct coupling at 9.3 GHz center frequency with series feeding method in both xz- and yz-planes [17].

In this paper, a new 3 × 3 patch planar array antenna prototype operating at 9.65 GHz for the airborne SAR applications is introduced. Dual-polarization operation can enhance the information content by providing two co- polarization and two cross polarization scatter data. The SIR-C shuttle imaging radar operated at L and C bands with dual polarization at each frequency, with a bandwidth of 10-20 MHz [18]. The proposed design offers a bandwidth Section II describes the details of the antenna requirements. The configuration of the proposed array antenna is presented and discussed in section II. In section fabricated and measured results are discussed for all individual ports. Finally, the conclusions of this work are given in Section IV.

II. ANTENNA GEOMETRY

The proposed antenna configuration is, 3 × 3 series-fed array. This 9.65GHz six-port 3 × 3 planar array consists of a 50Ω microstrip line direct coupling through the quarter wave transmission line ($\lambda_g/4$) to match the antenna impedance and series feeding for array and 6 square patch elements at the top layer. The square array geometry with patch elements with series feed line can miniaturize the antenna losses. A 31mil (0.787mm) thick with 1Oz i.e. 0.035mm thick copper Rogers RT/Duroid 5880 copper cladding substrate with relative permittivity $\varepsilon_r = 2.2$ and loss tangent tan d = 0.0009 is chosen as the antenna material [19]. Gold plated Amphenol RF Subminiature-A (SMA) male extended legs (Part no: 132134) connector was used to solder the microstrip

TABLE 1. Dimensions of antenna prototype.

Parameter	Description	Value (mm)
PL	Length of the patch	10
PW	Width of the patch	10
QTL	Length of the quarter wave transformer	2
QTW	Width of the quarter wave transformer	0.28
MTL	Length of the matching transformer	10.25
MTW	Width of the matching transformer	2.46
SFL	Length of the series-fed line	22
SFW	Width of the series-fed line	1.9
SUBL	Length of the substrate	80
SUBW	Width of the substrate	80
SUBH	Height of the substrate	0.787
BPL	Length of the brass plate	80
BPW	Width of the brass plate	80
BPT	Thickness of the brass plate	0.8
CPT-P	Thickness of the copper-patch	0.035
CPT-G	Thickness of the copper-ground	0.035
GPT-P	Gold plating thickness-patch	0.001
GPT-G	Gold plating thickness-ground	0.001

line feed. All simulations process are performed using CST Microwave Studio 2016 [20], an industry standard software simulator which is based on Finite Element Method (FEM) for frequency domain and FIT-Finite Integration Technique for time domain that is equivalent to FDTD-Finite Difference Time Domain.

A. THE GEOMETRY OF 6-PORT PLANAR ARRAY DESIGN

Fig.1 (a) shows the configuration of the 3 × 3 series fed with 6-ports planar array. The S_{11} shows the best case quarter wave transformer width (QTW = 0.28); Quarter wave transformer length (QTL = 2) ($\lambda_g = 24.57$; $\lambda_g/4 = 6.14$ with optimization for the resonant frequency of 9.65GHz the value of quarter-wave transformer is 2 mm which is approximately $\lambda_g/10$) and QTW = 0.28mm ($\approx 146\Omega$). This impedance variation is because of array environment. The effect of series feeding leads to impedance change in quarter wave transformer ($\lambda_g/4$). The nine square patches are connected to each other by series feeding in a 2-D manner using the lines with dimensions of SFW and SFL are 1.9mm and 20mm from the one patch feed point to another. To design a 0.7λ array in both XZ and YZ planes, the value of SFL was selected to be 20 mm which provides a scan angle of $\pm 25^0$ in the elevation plane from zenith angle of the upper hemisphere based on the equation (1-2). To improve the impedance matching between the elements the value of SFW was optimized to 1.9mm ($\approx 59\Omega$). Table 1 shows the dimensions of the designed prototype.

The optimization was done so that the array will have the maximum gain and good matching at broadside direction. The impedance bandwidth is from 9.52GHz to 9.76GHz for return loss S11 < −10dB. Also across the impedance bandwidth, the isolation is below −25 dB, with the isolation at the resonant frequency about −26 dB. By using the simulation software CST, simulated surface current distribution, in the microstrip line feed and radiating patch for the cases with QTL, QTW, MTL and MTW were obtained at resonant
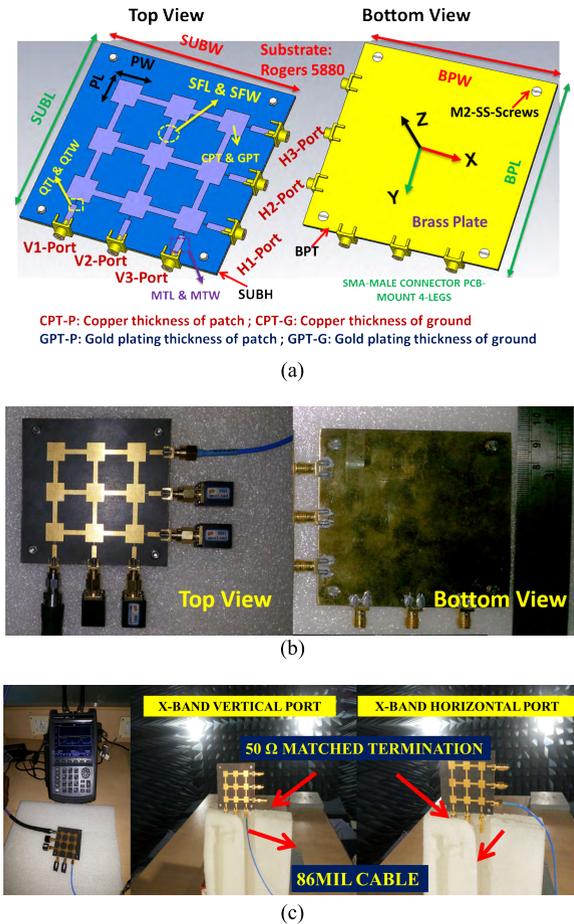
FIGURE 1. The geometry of the proposed 6-port 3 × 3 planar array (a) CST model (b) Fabricated prototype (c) S-parameters and radiation pattern measurement setup in anechoic chamber.
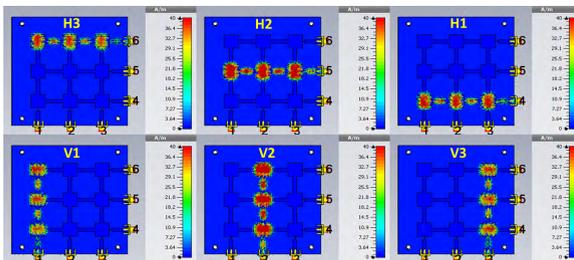
FIGURE 2. The surface current distribution at 9.65 GHz for all ports.

frequency 9.65 GHz and shown in Fig. 2.

$$d_x = \frac{\lambda_V}{1 + \sin \theta_x} \quad (1)$$

$$d_y = \frac{\lambda_H}{1 + \sin \theta_y} \quad (2)$$

dx = Inter-element spacing between the elements in x-direction

dy = Inter-element spacing between the elements in the y-direction

θ = Maximum scan angle, λ = free space wavelength at 9.65GHz

λ_V = free space wavelength in V-port

λ_H = free space wavelength in H-port
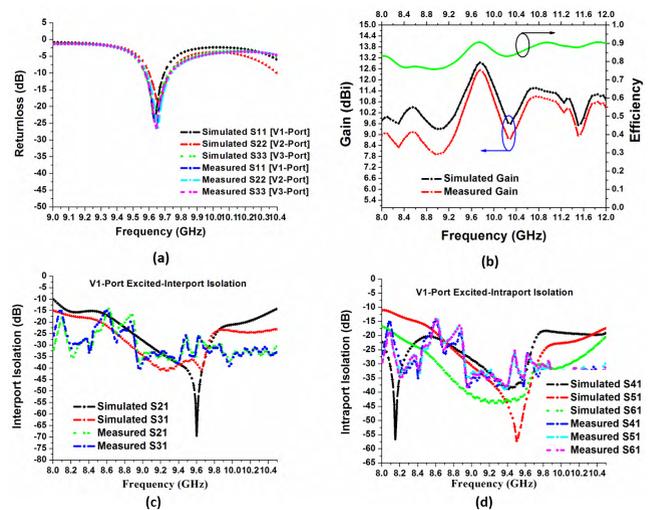
FIGURE 3. The simulated and measured (a) S-parameters (S11 & S21-S31-S41-S51-S61) at V1-port (all other ports are matched with 50Ω impedance terminations), (b) Gain and efficiency, (c) V1-Port excited-interport isolation, (d) V1-Port excited-intraport isolation.

III. FABRICATED AND MEASURED RESULTS

The X-band 6-port square patch array antenna with its center frequency 9.65 GHz has been fabricated and measured to validate the design. The fabricated prototypes with top and bottom views are shown in Fig. 1(b). The S-parameters are measured using Agilent N9918A field fox microwave analyzer and the radiation patterns and gain were measured in an anechoic chamber with a standard gain horn as reference antenna (supplier: Haining ocean import and export Co. Ltd) of 6m × 4m × 3m (L × W × H) with Agilent PNA series network analyzer N5230C (10MHz to 40GHz) Analyzer. The measurement setup for both S-parameters and radiation pattern are shown in Figure 1 (c). Following subsections deals with two cases for vertical and horizontal port excitations individually.

A. VERTICAL PORT-1 EXCITED

Fig. 3 shows the comparison between the simulated and measured S-parameters and gain of the proposed single port antenna. For V1-port the simulated return loss bandwidth S11 <-10 dB achieved is 9.59-9.71 GHz or 1.4 %, while the measured bandwidth results are in the range from 9.591-9.712 GHz or 1.4 % at the center frequency of 9.65 GHz. Fig 3(c-d) shows the port isolation lower than −25 dB interport isolation (S21 refers to V2-V1, S31 refers to V3-V1) and intraport isolation (S41 refers to H1-V1, S51 refers to H2-V1 and S61 refers to H3-V1). This is achieved with the selection of appropriate dimensions of quarter wave and matching transformer feeding position. The measured and simulated antenna gain and simulated efficiency against the frequency of the proposed antenna prototype at V1-port are shown in Fig. 3 (b). At the center frequency, V1-port achieves a peak antenna gain of 11 dBi with a gain variation of less than 0.2 dBi over the impedance bandwidth. By considering the simulated directivity and the
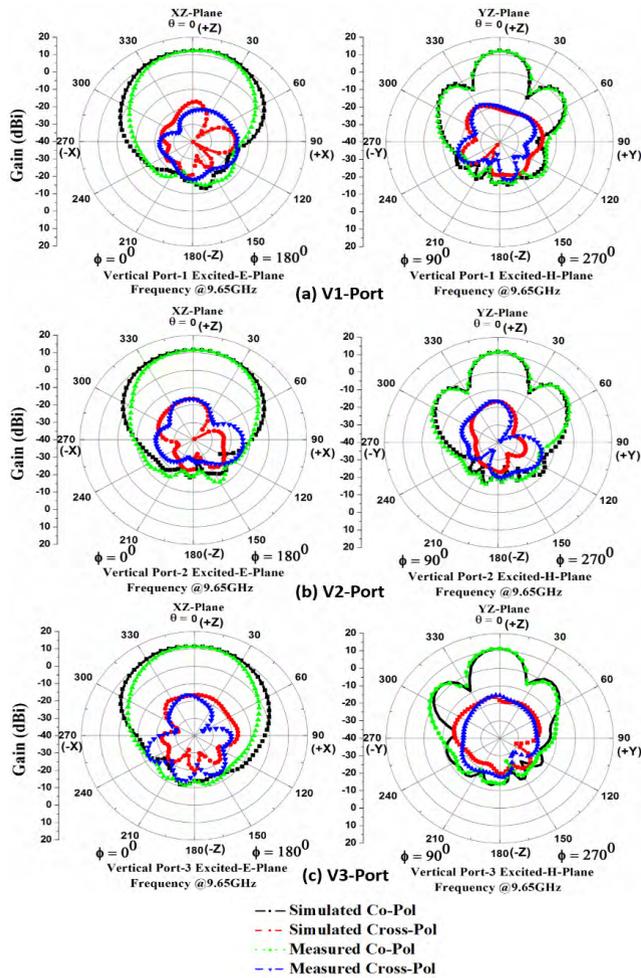
FIGURE 4. The simulated and measured radiation patterns terminations) (a) V1-Port E-Plane (XZ-Plane) and H-plane (YZ-Plane), (b) V2-Port E-Plane (XZ-Plane) and H-plane (YZ-Plane), and (c) V3-Port E-Plane (XZ-Plane) and H-plane (YZ-Plane).

measured gain the value of the measured radiation efficiency is about 90% over the impedance bandwidth. The measured results mostly agree and validate the results produced via simulations. A small discrepancy between the simulated and measured results may be caused by the error of the fabrication and assembling of the antenna. The S-parameters notations are given below

V1-Port : $|S_{11}| \leq -10dB$

$|S_{21}| \approx |S_{31}| \approx |S_{41}| \approx |S_{51}| \approx |S_{61}| \leq -25dB$

V2-Port : $|S_{22}| \leq -10dB$

$|S_{21}| \approx |S_{23}| \approx |S_{24}| \approx |S_{25}| \approx |S_{26}| \leq -25dB$

V3-Port : $|S_{33}| \leq -10dB$

$|S_{31}| \approx |S_{32}| \approx |S_{34}| \approx |S_{35}| \approx |S_{36}| \leq -25dB$

The measured and simulated radiation patterns in terms of the E-plane and H-Plane 2D polar plots are shown in Fig 4. Exciting RF antenna vertical port-1, it is observed that the E-plane with co-pol and cross-pol components has a main lobe magnitude of 12.5 dBi, Side lobe level of −25.4 dB, front to back ratio (FTBR) 32.83 dB and half-power beam
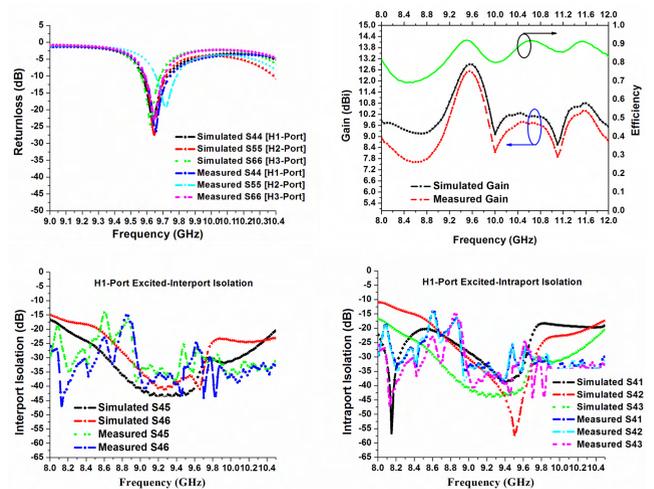
FIGURE 5. The simulated and measured (a) S-parameters (S11 & S41-S42-S43-S45-S46) at H1-port (all other ports are matched with 50Ω impedance terminations), (b) Gain and efficiency, (c) H1-Port excited-interport isolation, (d) H1-Port excited-intraport isolation.

width (HPBW) of 71.2^0 respectively. In contrast, the H-Plane with its co-pol and cross-pol components has a main lobe magnitude of 11.3 dBi, side lobe level of −10.2 dB, FTBR is higher than 32 dB and an HPBW of 25^0 respectively. The other antenna performance characteristics for V2-port and V3-port such as side lobe level (SLL), front-to-back (FTBR) ratio, gain, radiation and total efficiencies and cross-polarization level are calculated and summarized in Table 2.

B. HORIZONTAL PORT-1 EXCITED

Fig. 5 shows the measured S-parameters and gain at X-band in comparison with the simulated ones. It is observed that the measured results agree reasonably well with the simulations. For X-band operation, a measured bandwidth from 9.569 to 9.701 GHz (FBW = approximately1.4%) is achieved for the H2-port. At the center frequency of 9.65 GHz, the measured return losses are over 20 dB for all the three horizontal ports.

In the operation band, the measured isolation is less than −25 dB between the two ports/polarizations. Fig 5 (c-d) shows the port isolation reaching values higher than 25 dB interport isolation (S45 refers to H1-H2 and S46 refers to H1-H3) and intraport isolation (S41 refers to H1-V1, S42 refers to H1-V2, and S43 refers to H1-V3). The disagreements between the simulated and measured results at the three bands are mainly caused by the fabrication errors and the alignment tolerances.

H1-Port : $|S_{44}| \leq -10dB$

$|S_{41}| \approx |S_{42}| \approx |S_{43}| \approx |S_{45}| \approx |S_{46}| \leq -25dB$

H2-Port : $|S_{55}| \leq -10dB$

$|S_{51}| \approx |S_{52}| \approx |S_{53}| \approx |S_{54}| \approx |S_{56}| \leq -25dB$

H3-Port : $|S_{66}| \leq -10dB$

$|S_{61}| \approx |S_{62}| \approx |S_{63}| \approx |S_{64}| \approx |S_{65}| \leq -25dB$

The realized antenna gains and efficiency of the proposed antenna were presented in Fig. 5 (b). As shown in the figure,
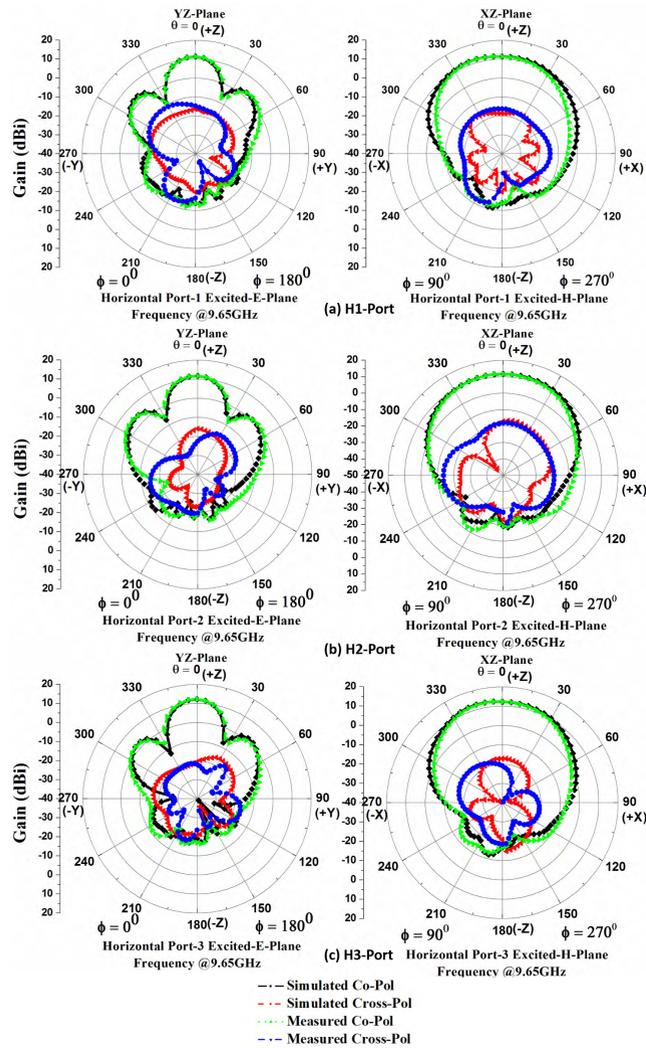
FIGURE 6. The simulated and measured radiation patterns for horizontal ports (a) H1-Port E-Plane (YZ-Plane) and H-plane (XZ-Plane), (b) H2-Port E-Plane (YZ-Plane) and H-plane (XZ-Plane), and (c) H3-Port E-Plane (YZ-Plane) and H-plane (XZ-Plane).

TABLE 2. Performance comparison.

Parameter		V1- Port	V2-Port	V3-Port
Band width		9.591-9.712	9.591-9.712	9.591-9.712
Gain(dBi)		12.1	11.5	11.7
Radiation efficiency(%)		91.1	89.4	90.6
E-Plane	SLL (dB)	-10.2	-11	-10.5
	HPBW (deg)	71.2	78.4	83.3
	Cross-pol (dB)	-28.1	-30	-30
	FTBR (dB)	32.83	32.83	32.83
H-Plane	SLL (dB)	-25.4	-25.9	-22.3
	HPBW (deg)	24.5	26.6	25
	Cross-pol (dB)	-28.1	-30	-30
	FTBR (dB)	32.83	32.83	32.83
Parameter		H1- Port	H2-Port	H3-Port
Band width		9.569-9.701	9.569-9.701	9.569-9.701
Gain(dBi)		11.3	11.5	12.2
Radiation efficiency(%)		90.6	89.4	91.1
E-Plane	SLL (dB)	-22.3	-25.9	-25.4
	HPBW (deg)	25	26.6	24.5
	Cross-pol (dB)	-30	-30	-30
	FTBR (dB)	31	31	31
H-Plane	SLL (dB)	-10.5	-11	-10.2
	HPBW (deg)	83.3	78.4	71.2
	Cross-pol (dB)	-30	-30	-28
	FTBR (dB)	31.8	31.8	31.8
Aperture area (Ap)		6400mm²		
Effective area (Ae)		4408.96mm²		
Aperture efficiency (ea)		68.89%		
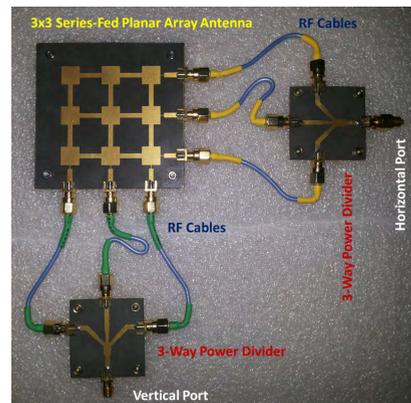
FIGURE 7. Combined V-ports and H-ports with 3-way power divider for maximum gain.

the measured gain curve shows reasonable agreement with the simulated gain curve. In the operational band (9.591-9.712 GHz), the simulated gains range from 11.3-12.5 dBi, while the measured gains range from 11.1-12.3 dBi.

The radiation patterns in the X-band are shown in Fig. 6 (a) (b) and (c), The measured gain can achieve 11.3 dBi (H-plane i.e. XZ-plane) and 12.1 dBi (E-plane i.e. YZ-plane) for broadside radiation in the X-band, respectively. The other antenna performance characteristics for H2-port and H3-port such as side lobe level (SLL), front-to-back (FTB) ratio, gain, radiation and total efficiencies and cross-polarization level are calculated and summarized in Table 2.

C. BEAM SCANNING MECHANISM

The combined V-port and H-port 3 × 3 planar array configuration is illustrated in Fig.7. The beam scanning is achieved by applying the different excitation phase values to the 3-input ports for vertical polarization and 3-input ports for horizontal

polarization. To study the beam scanning capability of the 3 × 3 array antenna and because of the symmetry, first all the ports are excited with zero degree phase and equal amplitude which results in a maximum gain equal to 19 dBi in the broad side direction ($\theta = 0^0$). Here the SLL is -23 dB at both E-plane and H-plane. Next, the phase of the vertical and horizontal ports are adjusted to 22.5^0, 45^0, and 67.5^0, (tilt angle $\theta = 5^0$), 45^0, 90^0, and 135^0(tilt angle $\theta = 10^0$), 67.5^0, 135^0, and 202.5^0(tilt angle $\theta = 15^0$), 90^0, 180^0, and 270^0 (tilt angle $\theta = 20^0$), and 112.5^0, 202.5^0, and 292.5^0(tilt angle $\theta = 25^0$), respectively are shown in Fig. 8. As an example, Fig. 9 shows the CST 3D beam obtained by changing 3 vertical port phase excitation values to maximize the gain at ($\phi = 0$ $\theta = 0$), ($\phi = 0$, $\theta = -25$) ($\phi = 0$, $\theta = 25$), whereas the plot (xz-plane) shown in Fig. 8 represents the gain maximization
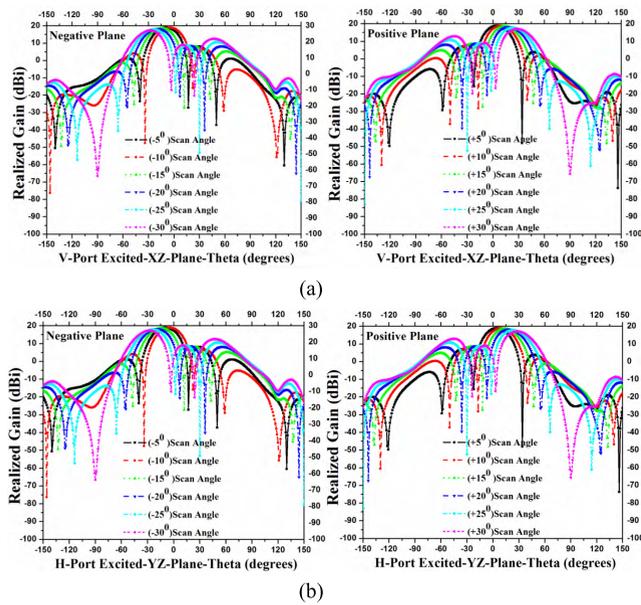
FIGURE 8. Scan angle patterns of xz-plane for different progressive phase shift (a) V-Polarization, (b) H-Polarization.
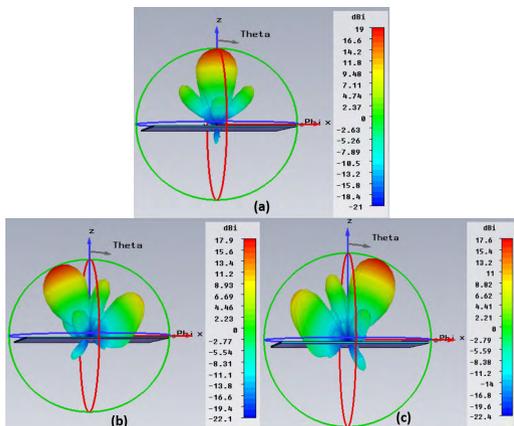
FIGURE 9. 3D far-field gain (a) Broadside direction ($\phi = 0^0$ & $\theta = 0^0$), (c) Elevation tilt angle ($\phi = 0^0$ & $\theta = -25^0$), (c) Elevation tilt angle ($\phi = 0^0$ & $\theta = +25^0$).

output at all these respective tilting angles. A gain variation of less than 1.4 dBi (17.6 to 19 dBi) has been observed over the tilt angle $\pm25^0$.

IV. CONCLUSION

In this paper, a new nine-element square patch array antenna design at 9.65 GHz for the airborne SAR applications has been introduced. In this paper, an X -band dual-polarized antenna array is presented. The square patch, microstrip line feeding for an element, and series feeding for an array are employed as a design of the 6-port 2D 3 × 3 planar array. The consideration of arranging the radiation elements as well as the feeding networks are detailed. To accommodate the six ports within a compact area, the techniques of microstrip line feed is adopted. The series feed network of the X-band is placed on the same layer. The proposed antenna array is optimized, fabricated and tested, showing a good impedance matching bandwidths of 1.4%, for all 6-ports at

X-band, respectively. The isolations between the two inter-port and intraport polarizations between all ports are around -25 dB. The antenna also exhibits an excellent radiation performance in terms of the side lobe, gain, efficiency, and cross-polarization. The advantages of the proposed antenna include low profile, low cost, high integration capability and easy in fabrication. A detailed comparison of performance between the all individual ports has been presented. The proposed array antenna is a good candidate for airborne SAR applications.

REFERENCES

[1] M. I. Skolnik, *RadarHandbook*. NewYork, NY, USA: McGraw-Hill, 1970.
[2] M. Fakharzadeh, M.-R. Nezhad-Ahmadi, B. Biglarbegian, J. Ahmadi-Shokouh, and S. Safavi-Naeini, "CMOS phased array transceiver technology for 60 GHz wireless applications," *IEEE Trans. Antennas Propag.*, vol. 58, no. 4, pp. 1093–1104, Apr. 2010.
[3] K. Zhao, J. Helander, Z. Ying, D. Sjoberg, M. Gustafsson, and S. He, "mmWave phased array in mobile terminal for 5g mobile system with consideration of hand effect," in *Proc. 81st IEEE VTC Spring*, May 2015, pp. 1–4.
[4] D. Ehyaie and A. Mortazawi, "A 24-GHz modular transmit phased array," *IEEE Trans. Microw. Theory Techn.*, vol. 59, no. 6, pp. 1665–1672, Jun. 2011.
[5] D. Ehyaie and A. Mortazawi, "A new approach to design low cost, low complexity phased arrays," in *IEEE MTT-S Int. Microw. Symp. Dig.*, May 2010, pp. 1270–1273.
[6] E. Topak, J. Hasch, C. Wagner, and T. Zwick, "A novel millimeter-wave dual-fed phased array for beam steering," *IEEE Trans. Microw. Theory Techn.*, vol. 61, no. 8, pp. 3140–3147, Aug. 2013.
[7] J. James and P. Hall, *Handbook of Microstrip Antennas* (IEEEElectromagnetic Waves Series 28), vol. 2. London, U.K.: Peregrinus, 1989.
[8] D. Pozar and D. Schaubert, "Comparison of three series fed microstrip array geometries," in *Proc. IEEE Antennas Propag. Soc. Int. Symp.*, Jun./Jul. 2002, pp. 728–731.
[9] F.-Y. Kuo and R.-B. Hwang, "High-isolation X-band marine radar antenna design," *IEEE Trans. Antennas Propag.*, vol. 62, no. 5, pp. 2331–2337, May 2014.
[10] T. Yuan, N. Yuan, and L. W. Li, "A novel series-fed taper antenna array design," *IEEE Antennas Wireless Propag. Lett.*, vol. 7, pp. 362–365, 2008.
[11] Y. I. Chong and D. Wenbin, "Microstrip series fed antenna array for millimeter wave automotive radar applications," in *Proc. IEEE MTT IMW*, Sep. 2012, pp. 1–3.
[12] P. Hallbjörner, I. Skarin, K. From, and A. Rydberg, "Circularly polarized traveling-wave array antenna with novel microstrip patch element," *IEEE Antennas Wireless Propag. Lett.*, vol. 6, pp. 572–574, 2007.
[13] T. R. Cameron, A. T. Sutinjo, and M. Okoniewski, "A circularly polarized broadside radiating 'herringbone' array design with the leaky-wave approach," *IEEE Antennas Wireless Propag. Lett.*, vol. 9, pp. 826–829, 2010.
[14] S. Karimkashi and G. Zhang, "A dual-polarized series-fed microstrip antenna array with very high polarization purity for weather measurements," *IEEE Trans. Antennas Propag.*, vol. 61, no. 10, pp. 5315–5319, Oct. 2013.
[15] M. Carter and E. Cashen, "Linear arrays for centimetric and millimetric wavelengths," in *Proc. 2nd Conf. Military Microw.*, vol. 1. 1981, pp. 315–320.
[16] R. Owens and J. Thraves, "Microstrip antenna with dual-polarization capability," in *Proc. Military Microw. Conf.*, 1984, pp. 250–254.

[17] V. K. Kothapudi and V. Kumar, "A single layer S/X-band series-fed shared aperture antenna for SAR applications," *Prog. Electromagn. Res. C*, vol. 76, pp. 207–219, Aug. 2017.

[18] R. L. Jordan, B. L. Huneycutt, and M. Werner, "The SIR-C/X-SAR synthetic aperture radar system," *IEEE Trans. Geosci. Remote Sens.*, vol. 33, no. 4, pp. 829–839, Jul. 1995.

[19] *RT/Duroid 5870/5880 High Frequency Laminates Available on the Internet.* Accessed: 2015. [Online]. Available: http://www.rogerscorp.com/documents/606/acm!RT-duroid-5870-5880-Data-Sheet.pdf

[20] Wellesley Hills, MA. (2016). *Computer Simulation Technology Version.* [Online]. Available: http://www.cst.com

VENKATA KISHORE KOTHAPUDI (S'14–M'18) was born in Tenali, India, in 1987. He received the degree in electronics and communication engineering from TPIST, JNTU, Hyderabad, India, in 2008, and the M.Tech. degree in communication and radar systems from the Koneru Lakshmaiah Education Foundation, India, in 2012. He is currently pursuing the Ph.D. degree with the Microwave Division, School of Electronics Engineering, VIT University, Vellore, India. He has over seven years of research and industry experience in RF and microwave engineering in ECIL as a GEA, NARL-ISRO as a Project Student, and Astra Microwave Products as an Engineer. He has a rich experience on radar systems design, which includes transmit/receive modules [HF-, VHF-, *L*-, *S*-, and *C*-band], RF and microwave feeder network and beam forming, RF and microwave active and passive components, RF power amplifiers, and antenna system, which includes the Yagi-Uda and the microstrip patch antennas as a phased array with different configurations by using analysis and synthesis techniques. He has published over 15 research papers in international journal and national and the IEEE international conferences. He has authored and co-authored of many IEEE proceeding papers. His area of research interests include shared aperture antenna technology for radar engineering includes airborne and space borne synthetic aperture radar and radar wind profilers. He is a member of AIAA and ACES.

VIJAY KUMAR (S'08–M'12) received the M.Sc. degree in physics (electronics) from Magadh University, India, in 2003, the M.Tech. degree in microwave remote sensing from BIT Mesra, Ranchi, in 2005, and the Ph.D. degree in engineering from IIT Bombay, Mumbai, in 2011. He was with DST, Government of India, a sponsored Scientist with IIT Bombay from 2009 to 2012. He is currently an Associate Professor with VIT University, Vellore, India. He has authored and co-authored of many peer-reviewed journal paper and over 20 proceeding papers. His research interests include radiating system designs for radar applications and miniaturized antenna designing using metamaterials. He has also been concentrating on SAR processing algorithm development, InSAR techniques, and SAR image processing, and pattern recognition. He is a member of AGU and SPIE, and a Life Member of ISRS.

• • •